



# City Research Online

## City St George's, University of London

**Citation:** Sun, Z. & Bruecker, C. (2017). Vortex ring impingement measured by scanning PIV. Paper presented at the 12th International Symposium on Particle Image Velocimetry, 18-22 Jun 2017, Busan, South Korea.

This is the accepted version of the paper.

This version of the publication may differ from the final published version. To cite this item please consult the publisher's version.

**Permanent repository link:** <https://openaccess.city.ac.uk/id/eprint/21654/>

**Copyright and Reuse:** Copyright and Moral Rights remain with the author(s) and/or copyright holders. Copies of full items can be used for personal research or study, educational, or not-for-profit purposes without prior permission or charge, unless otherwise indicated, provided that the authors, title and full bibliographic details are credited, a hyperlink and/or URL is given for the original metadata page and the content is not changed in any way. For full details of reuse please refer to [City Research Online policy](#).

# A Vortex Ring Impinging on a Slid Plate Measured by Scanning PIV

Zhengzhong Sun\*, Christoph Bruecker

Department of Mechanical Engineering and Aeronautics, City University of London, London, UK  
zhengzhong.sun@city.ac.uk

## ABSTRACT

Study on the impingement of a vortex ring onto a plate started a few decades ago [1]. This phenomenon is fundamental to several applications, such as the jet flow impinging on a wall, where vortex-wall interaction and heat transfer are of great interests. A few experimental as well as numerical researches have been carried out so far. A secondary ring with opposite rotation from the primary (original) vortex ring is found to be generated and azimuthal instability first takes place at the secondary ring. Following undulation of the secondary ring filament, interaction between the two rings occurs, which rapidly diffuse the coherent vortical structures into turbulent eddies in much smaller scale. The present experimental work is another attempt on this process and aims at providing a quantitative time-resolved representation of the impingement process, while special attention is paid to the instability phenomenon associated with the induced secondary vortex ring.

The scanning PIV measurement is carried out using the setup shown in figure 1. A glass water tank with internal dimension of  $30 \times 30 \times 48$  (W $\times$ L $\times$ H)  $\text{cm}^3$  is used as container. The vortex ring is produced through a piston-nozzle mechanism at the top of the tank. The cylindrical piston has a diameter of 30 mm and it is driven by a LinMot linear motor. In the experiment, the nozzle outlet is submerged in the water. The glass flat plate with size of  $20 \times 20$  cm is installed 20 cm below the nozzle outlet. A first surface mirror is further placed at  $45^\circ$  inclination below the glass plate so as to reflect the illuminated FOV into the camera in horizontal position. The flow illumination is provided by a 5W continuous laser at wavelength of 532 nm and the output beam has diameter of about 3 mm. The scanning light sheet is formed by the beam scanning technique using the drum scanner originally proposed by Bruecker [2]. In the present experiment, the twenty mirrors in the rotating drum are arranged in the dual-scan mode, thus a total of 10 light sheets are formed. The vertical distance of the first light sheet (closest to the plate) and the last light sheet (further to the plate) is 50 mm. The first laser sheet is placed at the surface of glass wall, thus the last light sheet is about 50 mm above the glass plate. The spacing for each two adjacent light slices are adjusted identical, namely 5.6 mm. The flow is recorded by a Phantom Miro310 high speed CMOS camera with  $1200 \times 800$  pixels sensor. The camera is equipped with a Sill telecentric lens. The lens aperture is set  $f_{\#}=11$ , allowing 6 planes from the wall are within the depth of focus while sufficient light intensity for PIV processing can be achieved. The imaging resolution is later calculated to be 0.08 mm/pixel. The camera is synchronized with the scanner. Since the motor driving the scanner operates at 3000 rpm, as a result the camera also operates at 1000Hz and the recording rate for each slice is therefore 200 Hz.

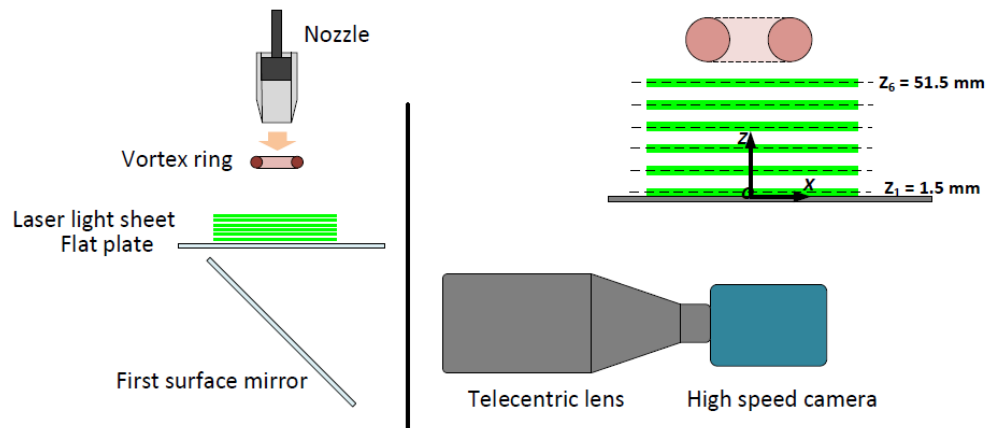


**Figure 1** The conceptual experimental setup and the arrangement of light sheets (top right).

The resulted vortex ring has a radius of  $R=43.5$  mm and it travels downward at speed of 55 mm/s. The PIV vector calculation of the present dataset has the final interrogation window of  $48 \times 48$  pixels with 50% overlap. The output vector thus has a total of  $53 \times 33$  vectors. The maximum particle displacement in the vortex ring before impingement is about 10 pixels. The vortex ring passes through plane 4 and plane 6 at  $T=3.397$  s before impingement. The maximum radial velocity is  $\pm 160$  mm/s and no significant azimuthal instability can be observed in the present vortex ring.

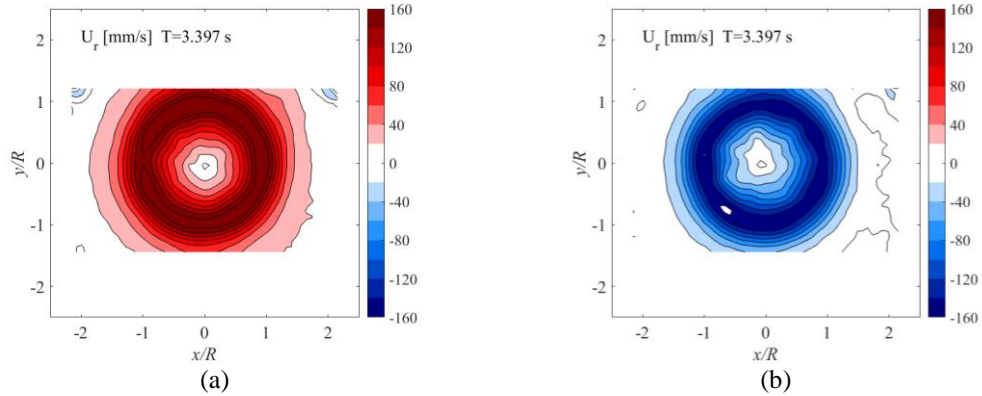


Figure 2 The radial velocity at plane 4 and plane 6 at  $T=3.397$  s: (a) plane 4 (b) plane 6.

The induced secondary vortex ring is also captured in the measurement. Azimuthal instability associated with the secondary vortex ring is revealed in plane 4 at  $T=4.437$  s (figure 3(a)). The unstable wave is represented by the packets containing alternating radial velocity. It is observed that the secondary ring has a larger radius of  $1.5R$  and a wave number of 8. At  $T=4.637$  s, the secondary ring shrinks as its diameter is only about  $1.0R$  (figure 3(b)). In the lower position, namely plane 3 (figure 3(c)), both the secondary and the original vortex ring are visualized together. The original ring (indicated by solid circle) featured by the negative radial velocity has radius of about  $1.8R$  due to the expansion caused by impingement. The secondary ring (indicated by the dashed circle) with apparent undulation is wrapped by the original ring. Following the progression of the instability activity at the secondary ring as well as its downward motion, the interaction between the two rings is initiated, which eventually dissipate the coherent vortical structures.

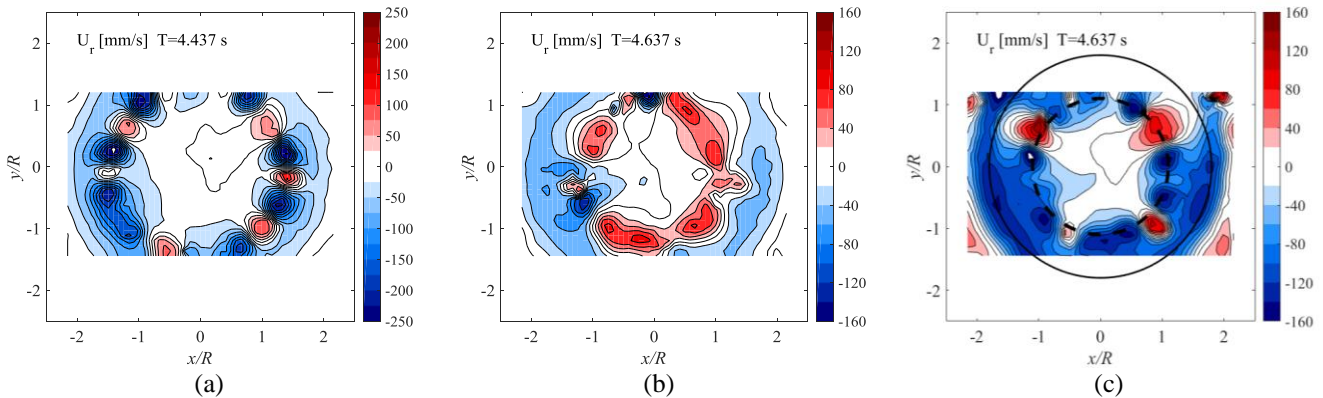


Figure 3 The secondary vortex ring evolution represent by radial velocity (a) plane 4 at  $T=4.437$  (b) plane 4 at  $T=4.637$  (c) plane 3 at  $T=4.637$ .

## REFERENCES

- [1] Walker JDA, Smith CR and Cerra AW "Impact of a vortex ring on a wall" J Fluid Mech. 181(1987) pp.99-140
- [2] Brücker C "3D scanning PIV applied to an air flow in a motored engine using digital high-speed video" Meas. Sci. Technol. 8(1997) pp.1480-1492.